



# Development of ketoprofen-*p*-aminobenzoic acid co-crystal: formulation, characterization, optimization, and evaluation

Meenakshi Bhatia<sup>1</sup> · Ashwani Kumar<sup>1</sup> · Vikas Verma<sup>2</sup> · Sunita Devi<sup>1</sup>

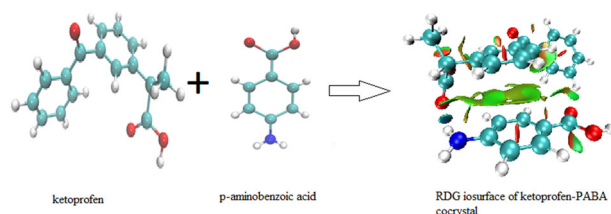
Received: 5 June 2021 / Accepted: 2 September 2021 / Published online: 20 September 2021

© The Author(s), under exclusive licence to Springer Science+Business Media, LLC, part of Springer Nature 2021

## Abstract

In the present study, ketoprofen-*p*-aminobenzoic acid (KP-PABA) co-crystal was prepared, to advance solubility and dissolution rate of drug, by solvent evaporation technique employing central composite experimental design. The optimized batch as recommended by the experimental design was characterized by FTIR, DSC, XRD, SEM, and NMR studies and further, evaluated for in-vitro and in-vivo anti-inflammatory and analgesic activities. The solubility and % drug release of different batches of co-crystal was found to be between 34.20–60.11 µg/ml and 68.11–93.45%, respectively. Physical characterization by X-ray diffraction spectra and differential scanning calorimetric studies confirmed the crystallinity of prepared co-crystal. The IC<sub>50</sub> value of optimized batch of co-crystal formulation and pure drug was observed as 248.79 µg/ml and 524.40 µg/ml, respectively, displaying that co-crystal formulation possesses more percentage protection against protein denaturation than the drug ketoprofen. The results of in-vivo anti-inflammatory activity carried out by rat paw edema method revealed that the optimized batch of co-crystal preparation provided a significant % inhibition in paw volume in contrast to standard drug in wistar rats. Hence, the crystalline molecular complex of ketoprofen with *p*-aminobenzoic acid was documented that set out an improvement in solubility and also in anti-inflammatory activity of the drug in wistar rats.

## Graphical Abstract



**Keywords** Ketoprofen · *p*-aminobenzoic acid · Co-crystal · Solubility enhancement · Solvent evaporation

## Introduction

Co-crystal is described as a multicomponent crystalline material possessing two or more molecules (i.e., drug and

coformer) that are connected by noncovalent interactions in the same crystal lattice [1, 2]. Co-crystal have the ability to improve the drug dissolution, bioavailability, hygroscopicity, solubility, processability, and physical/chemical stability of the compound as compared to active pharmaceutical ingredient (API) [3, 4]. Co-crystallization is an advanced method to improve pharmaceutical solid dosage form. The preference of a method to produce co-crystal is crucial and depends on different factors for example thermal stability, alteration in solubility of coformers and API in particular solvents, tendency to form stable polymorphs or solvates and availability of a sufficient amount of the substance [5]. The selection of suitable coformer for co-crystallization is based on aqueous

✉ Sunita Devi  
sunitamechu1504@gmail.com

<sup>1</sup> Departmental of Pharmaceutical Sciences, Guru Jambheshwar University of Science and Technology, Hisar 125001, India

<sup>2</sup> Departmental of Chemistry, Guru Jambheshwar University of Science and Technology, Hisar 125001, India

solubility of coformer, hydrogen bonding, noncovalent bonding, carbon-chain length and molecular recognition. The difference between pKa value of API and coformer (i.e.,  $\Delta pK_a$ ) also depicts the co-crystal formation capability of a coformer with a given API [6, 7]. According to Berry and Steed, salt formation occurs when  $\Delta pK_a$  value remains in close proximity to that of a base however co-crystal will be formed if this value exists close to acid [8]. The formation of co-crystal is formed if multiple H-bonds are formed [9, 10]. For instance, co-crystal of various drugs with different cofomers are listed as ketoconazole with *p*-aminobenzoic acid and nicotinamide, telmisartan with chitosan, aceclofenac with chitosan, tadalafil with methylparaben, carbamazepine with nicotinamide, piroxicam with PEG 4000, PVP K30, acetazolamide with theophylline and piperazine and 5-fluorouracil with gentisic acid, 3,4-dihydroxybenzoic acid and 4-aminopyridine that have been synthesized employing different techniques that contain solvent evaporation [11], solvent change approach [12, 13], solvent drop grinding [14], solution cooling crystallization, solvent evaporation, melting and cryomilling [15], slow crystallization [16], liquid-assisted grinding and solvent evaporation [17], solvent-assisted grinding and solution crystallization [18] etc.

Ketoprofen ( $C_{16}H_{14}O_3$ ) belongs to BCS-II, is a propionic acid derivative and can be taken orally to treat inflammatory diseases for instance rheumatoid arthritis, osteoarthritis, musculoskeletal disorders or postoperative pain [19]. The anti-inflammatory property of ketoprofen is due to inhibition of enzyme cyclooxygenase-I and II, thus curtailing the formation of precursors of prostaglandins and thromboxanes. The average half-life of ketoprofen elimination from human plasma is 2–4 h. It reaches the highest plasma concentration in 1–2 h. Plasma protein binding is ~99%. Oral absorption of the drug is almost complete, with bioavailability of 90% [20]. Several methods of improving the solubility or dissolution rate of ketoprofen have been put forward like solid dispersion [21, 22], Micronization [23], lquisolid [24], microemulsion-based gel [25], emulgels [26], nanoparticles [27, 28], solid lipid nanoparticles (SLNs) [29], prodrug with pectin [30], micro and nano-composite with PLGA [31] etc. Although the co-crystal of ketoprofen with conformer nicotinamide are known [32]. The above-mentioned techniques are associated with one or more drawbacks like instability during storage, tacky product, agglomeration, requirement of advanced/or sophisticated instruments etc. Therefore, co-crystal is opted being a simple, feasible, and cost-effective method, sometimes green as well. The mechanism involved in solubility enhancement by co-crystal “Maheshwari et al. [33] reported that solubilization of a co-crystal in dissolution medium involves two main steps: (1) Release of the solute molecules from the crystal lattice of the cocrystal and (2) the solvation of the released molecules. Therefore, free energy of co-

crystal solubilization depends on the free energy associated with the release of solute molecules from the cocrystal lattice and the free energy associated with the solvation barrier of the co-crystal as given in Eq. (1)

$$\Delta G_{\text{solution}} = \Delta G_{\text{lattice}} + \Delta G_{\text{solvation}} \quad (1)$$

where  $\Delta G_{\text{solution}}$  is the Gibb's free energy associated with the solubilization process,  $\Delta G_{\text{lattice}}$  is the Gibb's free energy associated with the co-crystal lattice and  $\Delta G_{\text{solvation}}$  is the Gibb's free energy associated with the solvation barrier. When the free energy associated with the lattice interactions and the free energy associated with the solvation barrier becomes negligible, enhancement in co-crystal dissolution is achieved due to decrease in free energy change for solubilization. The co-crystal formed with a highly water-soluble coformer, was found to possess high solubility. Therefore, solvation is the most important barrier for the solubilization of co-crystals for hydrophobic drugs [34].”

*P*-aminobenzoic acid (PABA) as a coformer purposed in this study is a member of the vitamin B complex and is generally recognized as safe (GRAS) [35]. The ketoprofen and PABA were selected on the basis of the pKa rule. Benzoic acid has pKa value of 4.21 whereas pKa value for ketoprofen is 3.88 and the difference in pKa value *i.e.*  $\Delta pK_a$  ( $pK_{a_{\text{acid}}} - pK_{a_{\text{base}}}$ ) is  $-1.36$  and according to Bhogala et al., at negative values of  $\Delta pK_a$ , co-crystal development is predictable [36].

In the present piece of research-work, easy and consistent technique of solvent evaporation was employed for composing the ketoprofen-PABA co-crystal seeking improved dissolution of drug. The preparation of co-crystal was accomplished as per central composite experimental design (CCD) by experimental design protocol selecting 2-factors at 3 levels (Design Expert software version 11.0). DSC, FT-IR, XRD, SEM, and NMR studies were utilized to characterize the optimized formulation. The optimized formulation was further evaluated for both in-vitro and in-vivo activities.

## Results and discussion

The preparation of co-crystal using ketoprofen and PABA was optimized using 2-factor, 3 level CCD. The concentration of ketoprofen ( $X_1$ ) and concentration of PABA ( $X_2$ ) were designated as independent variables whereas the % drug release and solubility ( $\mu\text{g/ml}$ ) were specified as dependent/response variables. Formulation parameters and responses for experimental design for different batches of KP-PABA co-crystal are exhibited in Table 1. The TDC of different batches of KP-PABA co-crystal was observed between 97.01 and 98.92%. No physical changes were observed during stability studies even after six months. In different batches of

**Table 1** Formulation parameters and responses for experimental design

Batch	Conc. of Ketoprofen (mg) (X <sub>1</sub> )	Conc. of PABA (mg) (X <sub>2</sub> )	Solubility in distilled water (µg/ml) (Y <sub>1</sub> )	Solubility in PBS pH-7.4 (µg/ml)	% In-vitro drug release in 60 min (Y <sub>2</sub> )	Total drug content (%)	ΔG (KJ/MOL)
1	508.58	137.14	45.02 ± 0.18	19.26 ± 0.014	79.47 ± 0.33	97.78 ± 0.13	-2.85
2	381.43	205.71	53.42 ± 0.3	28.36 ± 0.02	85.12 ± 0.36	98.42 ± 0.04	-3.34
3	381.43	274.28	58.14 ± 0.2	33.39 ± 0.08	85.69 ± 0.22	97.12 ± 0.08	-3.66
4	381.43	205.71	53.12 ± 0.21	27.58 ± 0.01	82.94 ± 0.41	97.94 ± 0.06	-3.30
5	381.43	205.71	55.19 ± 0.19	31.47 ± 0.04	79.80 ± 0.34	97.91 ± 0.08	-3.43
6	381.43	137.14	42.32 ± 0.22	15.96 ± 0.02	69.74 ± 0.8	97.70 ± 0.03	-2.66
7	508.58	274.28	60.11 ± 0.26	35.16 ± 0.032	93.45 ± 0.15	98.92 ± 0.02	-3.51
8	381.43	205.71	52.23 ± 0.27	26.27 ± 0.014	83.87 ± 0.09	98.06 ± 0.04	-3.41
9	508.58	205.71	56.63 ± 0.33	32.33 ± 0.015	85.86 ± 0.096	98.14 ± 0.06	-3.48
10	254.29	205.71	49.71 ± 0.8	24.44 ± 0.023	75.90 ± 0.05	97.91 ± 0.03	-3.13
11	254.29	137.14	34.20 ± 0.9	11.42 ± 0.025	68.11 ± 0.73	97.78 ± 0.01	-2.07
12	254.29	274.28	50.16 ± 0.6	25.67 ± 0.015	83.77 ± 0.72	97.01 ± 0.03	-3.17
13	381.43	205.71	52.58 ± 0.13	26.18 ± 0.03	88.11 ± 0.77	98.90 ± 0.06	-3.32
Ketoprofen			14.94 ± 0.3	4.52 ± 0.017	22.79 ± 0.56		

All values are expressed as mean ± S.D.,  $n = 3$

KP-PABA co-crystal solubility in phosphate buffer (PBS pH-7.4) values range from 19.26 to 35.16 µg/ml whereas ketoprofen solubility was found to be 4.52 µg/ml.

### Solubility studies

The outcome of solubility ( $Y_1$ ) and in-vitro drug release profile ( $Y_2$ ) of the KP-PABA co-crystal, formulated according to the experimental design expert protocol is exhibited in Table 1. The responses generated were fitted into numerous polynomial models.

The responses, solubility ( $Y_1$ ) and in-vitro drug release ( $Y_2$ ) were fitted best into the quadratic response surface model with none transformation of the data. In different batches of KP-PABA co-crystal solubility values range from 34.20 to 60.11 µg/ml and % in-vitro drug release range for 68.11–93.45%. This upheave in solubility and thus dissolution may be due to the formation of soluble complex between ketoprofen and PABA. The solubility of KP-PABA co-crystal (60.11 µg/ml) was higher than that of the ketoprofen (14.94 µg/ml). The reason for this furtherance in solubility is the intermolecular hydrogen bonding between the ketoprofen and PABA and it is surmised that this linkage may result in hydration of co-crystal and thereby, the high solubility of the drug is observed from co-crystal.

The polynomial models for the responses solubility ( $Y_1$ ) and in-vitro drug release ( $Y_2$ ) can also be expressed by the Eqs. (2) and (3), respectively. The synergistic and antagonist effect is explained by the positive and negative coefficient value for specific independent variables in the polynomial Eqs. (2) and (3). The equations generated

revealed that both factors independently exerted a significant effect on the solubility and in-vitro drug release. The response surface plots (Fig. 1a, b) revealed that solubility and in-vitro drug release vary in curvilinear fashion with an increase in the amount of each factor. However, the effect of the concentration of PABA ( $X_2$ ) seems to be more pronounced as compared with that of the concentration of ketoprofen ( $X_1$ ).

$$Y_1 = 53.68 + 4.61X_1 + 7.81X_2 - 0.275X_1X_2 - 1.45X_1^2 - 4.39X_2^2 \quad (2)$$

$$Y_2 = 42.218 + 0.037X_1 + 0.119X_2 - 0.317X_1X_2 - 3.51X_1^2 - 3.31X_2^2 \quad (3)$$

The denouement of ANOVA test on the response surface quadratic model are summarized in Table 2, demonstrated that the model was found significant with lack of fit as non-significant. A good correlation among experimental and predicted responses was specified with a good value of  $R^2$  (>0.9). The adequate precision measuring signal to noise ratio (greater than 4) is desirable. In this design, the ratio of 25.49 (solubility) and 23.05 (drug release) illustrated an adequate signal that let the model to navigate design space. Figure 1a, b displays the combined effect of concentration of ketoprofen & PABA on solubility and drug release. It can be interpreted from the plots that independent and dependent variables exists in a curvilinear correspondence. It is also inferred from the plot that higher level of ketoprofen & PABA results in increase in solubility of the formulation.

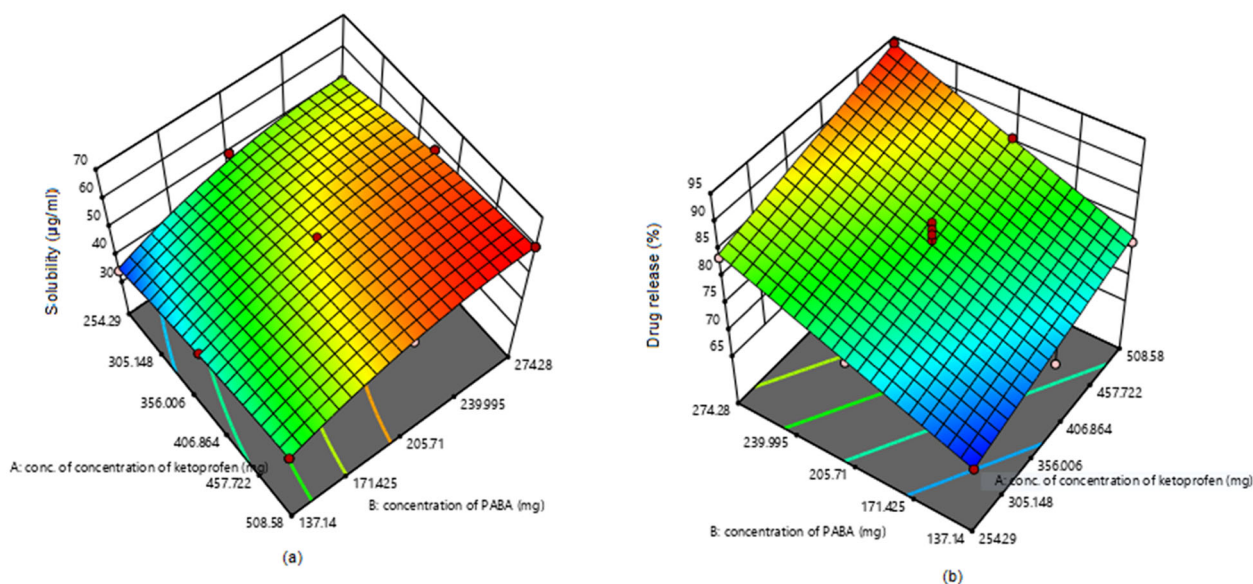


**Fig. 1** a, b Response surface plots displaying effect of concentration of ketoprofen (KP) & PABA on solubility ( $Y_1$ ) and in-vitro drug release ( $Y_2$ )

**Table 2** Model summary statistics

Response factors (Y)	F value	Prob. > F	R <sup>2</sup>	Adequate precision	C.V (%)	Lack of fit	
						F value	Prob. > F
Y <sub>1</sub>	20.58	<0.0001	0.975	25.49	2.81	2.31	0.218
Y <sub>2</sub>	49.19	<0.0001	0.907	23.05	2.88	1.56	0.34

To attain stability a natural tendency to acquire minimum Gibbs energy is always there. All the values of  $\Delta G$  are negative (Table 1) at all levels of carrier demonstrating spontaneity of drug solubilization process

### Optimization

The optimization Eqs. (2) and (3), relating the responses and independent factors, were acquired based on a quadratic model. To the responses *i.e.* solubility and in-vitro drug release the desirability function was applied with constraints to obtain the higher magnitude of both the factors. In this manner, the formulation containing PABA (274.28 mg) as cofomer and drug (508.58 mg) with addition of acetic acid (2%) solution at 60°C, established the maximum desirability, was organized and evaluated.

The optimization of independent variables was done with constraints of maximum solubility and maximum % release. The different set of solutions were provided by the optimization tool in the software (Design Expert software, version 11.0). The parameters suggested by the design were concentration of ketoprofen (508.58 mg) & concentration of PABA (274.28 mg) that provided co-crystal with solubility of 60 µg/ml (predicted value 60.051 µg/ml) and % release 93.45% (predicted value 93.94%). The closer concordance between observed and predicted values discerned high predictive ability of the model. Figure 2 displays the in-vitro release profile of

ketoprofen as pure drug and the optimized batch of the formulation.

The release profile of co-crystal is compared with equivalent concentration of pure drug solution to study release rate kinetics. The release of ketoprofen from co-crystal formulation and drug solution was put into various kinetic models to estimate the kinetics and mechanism of release (Table 3). The release rate data for the formulation was found to be fitted best into Zero-order model of release kinetics ( $R^2 = 0.951$ ). Further, the value of 'n' > 1.0 ( $n = 1.4$ ) the release exponent of Korsmeyer–Peppas equation indicated that the release of ketoprofen from co-crystal occurs by supercase-2 transport *i.e.* the release occurred by relaxation or erosion of polymer after swelling in biological fluids.

### FTIR spectroscopy

FTIR is an analytical method used to study the changes in the position caused by the vibration modes of the functional groups. The FTIR spectra revealed the shift in characteristic peaks of drug and co-former due to co-crystal formation involving H-bonding between the

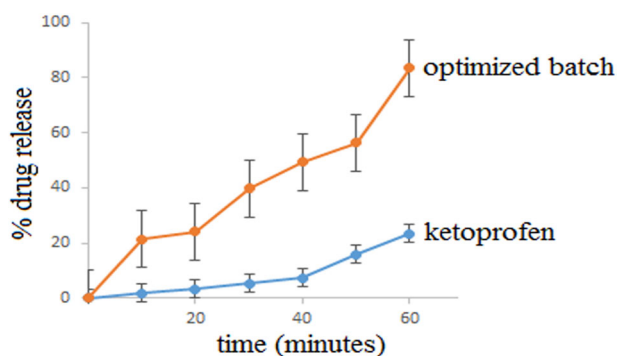


**Fig. 2** In-vitro release profile of pure drug (Ketoprofen) and KP-PABA co-crystal (optimized batch)

corresponding functional groups. The spectra of ketoprofen Fig. 3a showed characteristic absorption band at  $2979.27\text{ cm}^{-1}$  due to  $-\text{CH}$  stretching. The peak appearing at  $1697.76\text{ cm}^{-1}$  can be ascribed to  $-\text{C}=\text{O}$  stretching of acid while peak appearing at  $1655.77\text{ cm}^{-1}$  is due to  $-\text{C}=\text{O}$  stretching of ketone. The absorption bands at  $1598.67\text{ cm}^{-1}$  ( $-\text{C}=\text{C}$ -stretching),  $1442.21\text{ cm}^{-1}$  ( $-\text{C}=\text{O}$  stretching of aromatic ring),  $1420.59\text{ cm}^{-1}$  ( $-\text{C}-\text{H}$  deformation of  $\text{CH}_3$  asymmetrical) and  $1370.04\text{ cm}^{-1}$  ( $-\text{C}-\text{H}$  deformation of  $\text{CH}_3$  symmetrical) also appeared. The spectra of PABA presented the characteristic absorption band of  $-\text{NH}$  stretch appearing at  $3461.24\text{ cm}^{-1}$ , peak at  $3362.37\text{ cm}^{-1}$  is due to  $-\text{OH}$  stretch, peak

**Table 3** Modeling and release kinetics of ketoprofen from co-crystal

Formulation	Zero order $R^2$	First order $R^2$	Higuchi $R^2$	Korsmeyer–Peppas $R^2$ $n$
Drug solution	0.915	0.850	0.949	0.808 1.48
Co-crystal	0.921	0.813	0.932	0.913 1.52

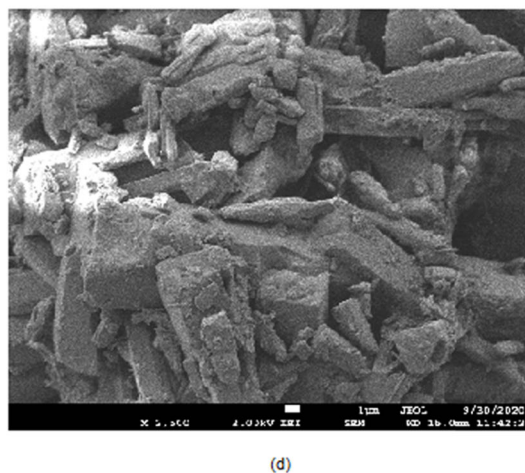
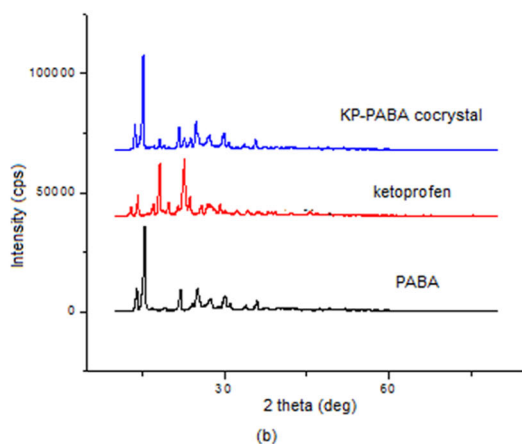
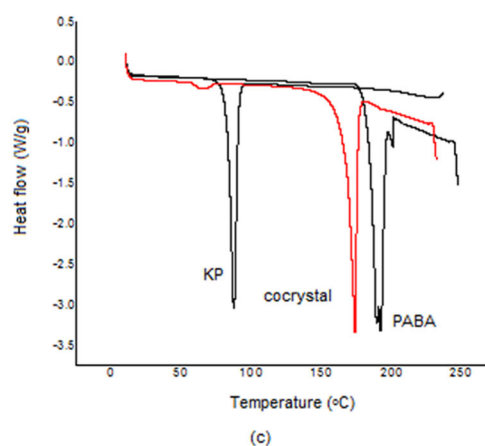
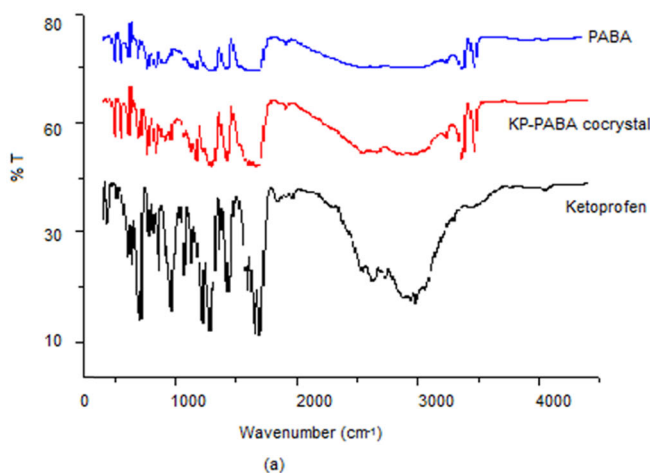


**Fig. 3** (a) FTIR, (b) XRD, (c) DSC spectra of ketoprofen, PABA and optimized batch of KP-PABA co-crystal, (d) SEM image of optimized batch of KP-PABA co-crystal

at 1681.89 is attributed to  $\text{C}=\text{C}$  aromatic stretching while peak at  $1422\text{ cm}^{-1}$  may be ascribed to  $\text{C}-\text{C}$  aromatic stretching. In FTIR spectra of KP-PABA co-crystal the peak due to  $\text{C}=\text{O}$  stretching of  $\text{-COOH}$  group of ketoprofen shifted from  $1697.76\text{ cm}^{-1}$  to  $1664.16\text{ cm}^{-1}$ . There was shift in  $\text{-NH}$  stretch from  $3362.37\text{ cm}^{-1}$  (PABA) to  $3360.95\text{ cm}^{-1}$  (KP-PABA co-crystal). These observations suggested the formation of hydrogen bond between amino group of PABA and  $\text{-COOH}$  group of ketoprofen in KP-PABA co-crystal.

### Powder X-ray diffraction (PXRD)

The X-ray diffraction spectra of ketoprofen, PABA and optimized batch of KP-PABA co-crystal is illustrated in Fig. 3b. In diffraction spectra of ketoprofen the peaks (and Miller indices) appeared at  $2\theta$  of 12.74 (100), 18.52 (200), 22.85 (211), 24.00 (221), 26.32 (222), 28.92 (300) whereas, in XRD spectra of PABA the peaks (and Miller indices) appeared 15.33(121), 22.67 (211), 24.88 (221), 27.18 (222) and 30.65 (310) that manifested crystalline structure of ketoprofen and PABA, respectively. The major diffraction peaks at  $2\theta$ , 13.32 (100), 15.90 (121), 18.8 (200), 21.69 (210), 25.45 (221) and 27.19 (222) were also observed in PXRD spectra of co-crystal that portrayed crystalline nature of formulation this indicating that resultant product is also crystalline in nature [37]. Moreover, some characteristic peaks of ketoprofen at 12.74, 22.85, and 28.92 disappeared while some peaks at 24.00 and 26.32 shifted to 25.45 and 27.19, respectively. Besides this, few peaks of PABA at 22.67 and 30.65 disappeared and few peaks at 15.33, 24.88, and 27.18 shifted to 15.90, 25.45, and 27.19, respectively. These changes in the PXRD data of respective co-crystal from ketoprofen and coformer are suggestive of the formation of new forms.

### Differential scanning calorimetry (DSC)

DSC thermogram (Fig. 3c) of ketoprofen displayed a sharp single peak at  $94.5\text{ }^\circ\text{C}$  that corresponds to its melting point. The peak at  $187.8\text{ }^\circ\text{C}$  attributed to melting point of PABA. However, in the DSC curve of co-crystal, a single endothermic peak appearing at  $180\text{ }^\circ\text{C}$  suggested the presence of a new phase (co-crystal) different from the constitutional components. The modification in the melting point is due to the alteration in the crystal lattice of the drug in the presence of coformer, indicating that certain adaptation has occurred.

### Scanning electron microscopy (SEM)

The SEM image of the co-crystal formulation was depicted in Fig. 3d. The co-crystal showed good crystalline

characteristics. This crystalline characteristic of co-crystal was reinforced by the XRD data, as discussed earlier. The pores over the surface of the co-crystal may brace the imbibition of the solvent/biological fluids, consequently, increasing the solubility and bioavailability of ketoprofen as anticipated.

### NMR spectroscopy

Nuclear magnetic resonance spectroscopy is used to characterize the co-crystal by studying the chemical environment of their nuclei and hydrogen bonding and it also offers valuable information regarding interactions. In the NMR spectra of KP-PABA co-crystal, the carbonyl carbon of ketoprofen corresponding to 196.46 ppm and 140.13 ppm has shifted to 196.12 ppm and 142.23 ppm, respectively. A deviation in the carbonyl carbon of carboxylic group in PABA shifted from 173.84 ppm and 152.13 ppm to 175.52 ppm and 153.60 ppm, respectively (Fig. 4). This suggests an interaction between amino group of PABA and  $\text{-COOH}$  group of ketoprofen in KP-PABA co-crystal.

### Noncovalent interactions (NCI) analysis

Co-crystal involves no covalent modification of its constituents and different chemical constituents interact through noncovalent interactions [38]. In order to identify the type of interactions that may be present in the cocrystal of ketoprofen and PABA, the NCI analysis was carried out. The chemical structures of ketoprofen and PABA were retrieved from pubchem database [<https://pubchem.ncbi.nlm.nih.gov>]. The two structures were combined and the system was minimized with molecular mechanics force field. This minimized system was further minimized using new and more accurate PM7 method by taking value of  $g_{\text{norm}}$  as 0.001 in MOPAC [39]. Different properties like electron energy, nuclear repulsion energy, total energy, dipole moment, interatomic distance and bond angles etc. of the final minimized co-crystal were calculated by DFT using 6–31 G\* basis set in B3LYP method of Firefly [40]. The interactions were determined using Multiwfn [41] and VMD [42].

Reduced density gradient (RDG) calculations show that one hydrogen bond is formed between carbonyl oxygen of the ketoprofen and hydrogen atom of amino group of PABA. Aromatic rings of both the molecules stacked against each other through pi-pi stacking interactions. Carbonyl oxygen atom of PABA made weak interactions with hydrogen atoms of terminal phenyl ring of ketoprofen. These interactions are shown in Fig. 5a below:

Further, Hirshfeld surface mapped by electron density with promolecular approximation analysis was also

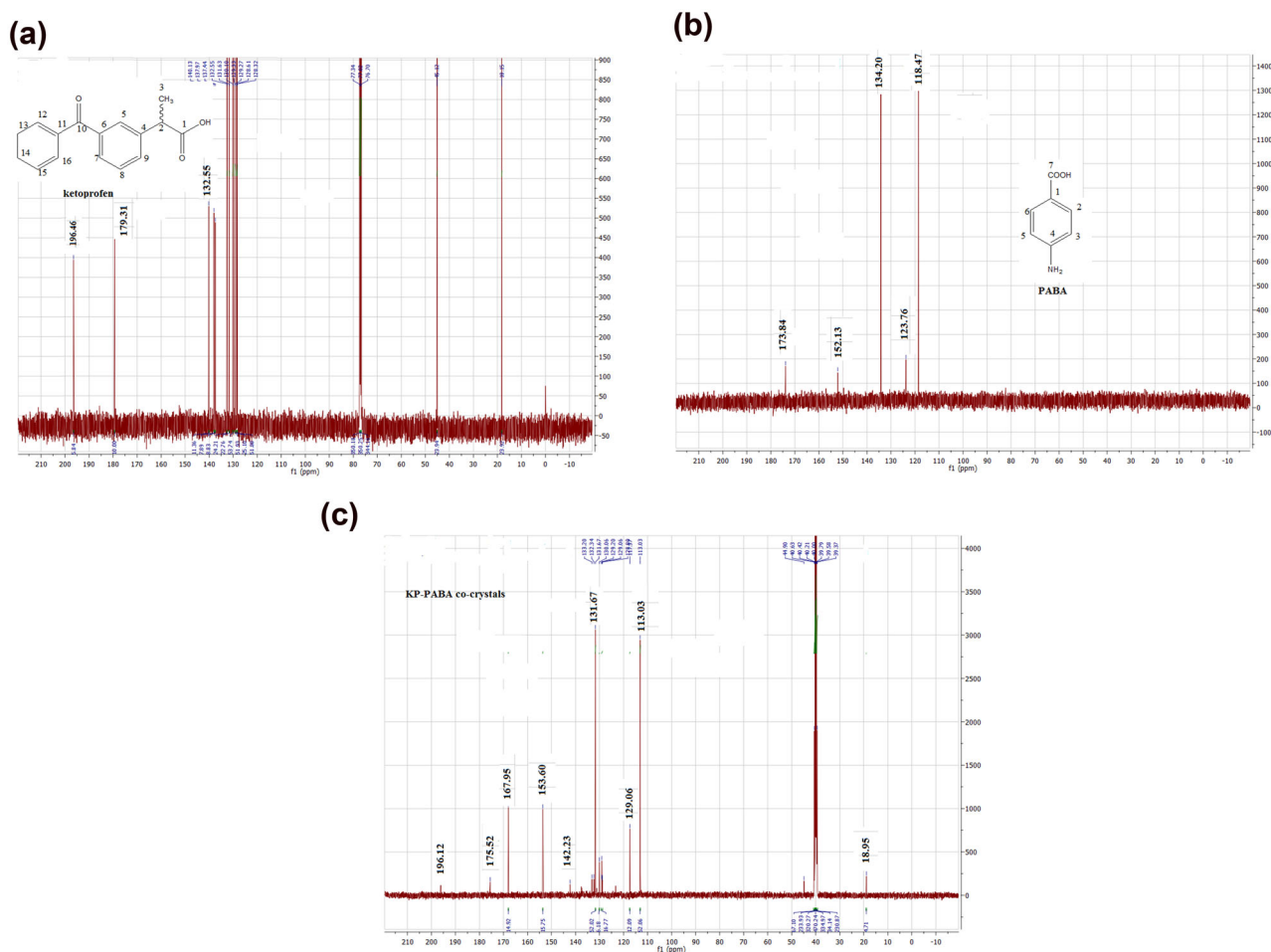
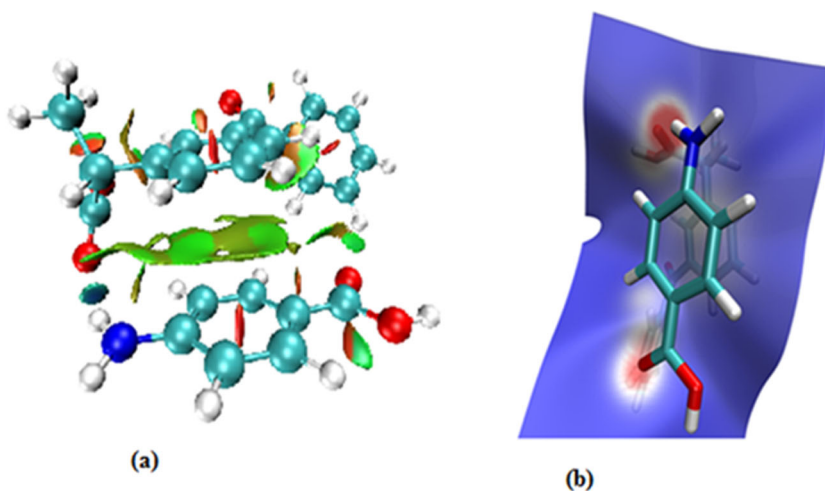


**Fig. 4** NMR spectroscopy of (a) ketoprofen, (b) PABA, and (c) KP-PABA co-crystal

**Fig. 5 a** RDG isosurface of ketoprofen-PABA cocrystal. Blue color indicates hydrogen bond and green and brown colors indicate weak Van der Waals interactions, **b** Hirshfeld surface mapped by electron density with promolecular approximation of ketoprofen-PABA co-crystal



performed to study the hydrogen bond and Van der waals interactions. Figure 5b shown here clearly indicates the region of high electron density in red color between PABA amino and ketoprofen carbonyl groups. Another one is

present between PABA carbonyl and terminal phenyl protons of ketoprofen whereas white region between two aromatic rings depicts lesser electron density means weaker interactions blue color indicates electron free region.

## Biological evaluation of KP-PABA co-crystal

### In-vitro anti-inflammatory activity

The comparison plot of % protection from protein denaturation at different concentration of optimized formulation and pure drug is shown in Fig. 6. The egg albumin method has shown a concentration-dependent significant anti-inflammatory activity by protection of protein. Pure drug and optimized KP-PABA co-crystal formulation at different concentrations have shown significant % protection. Non-linear regression analysis was used to calculate the half-maximal inhibitory concentration (IC<sub>50</sub>) values of ketoprofen and optimized formulation. The IC<sub>50</sub> values for ketoprofen are found to be 524.40 µg/ml and 248.79 µg/ml for optimized formulation. The IC<sub>50</sub> value of co-crystal formulation is almost half as compared to pure drug. Hence, it is concluded that co-crystal formulation is more active in producing anti-inflammatory response than the drug ketoprofen.

### In-vivo anti-inflammatory activity

Carrageenan-induced rat paw edema method was appropriated to compare oral efficacy of ketoprofen and optimized batch of KP-PABA co-crystal formulation. The improvement in activity of ketoprofen and co-crystal formulation was comparatively assessed by the increase in paw

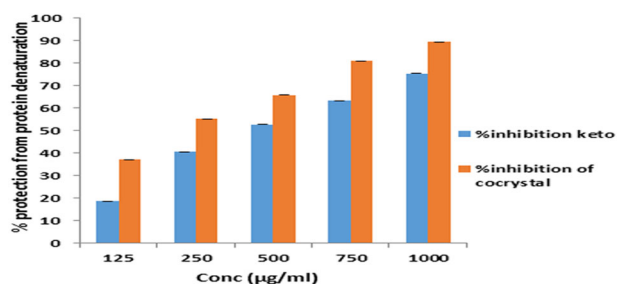


Fig. 6 % protection from protein denaturation of ketoprofen and optimized formulation

**Table 4** Effect of ketoprofen and ketoprofen-PABA formulation on the paw edema induced by carrageenan in Wistar rats

Time (min)	Paw volume (mm)			Inhibition (%)	
	Control	Pure drug	Co-crystal	Pure drug	Co-crystal
60	4.22 ± 0.01	4.06 ± 0.02 <sup>a</sup>	4.01 ± 0.01 <sup>a</sup>	3.73 ± 0.03	4.77 ± 0.05 <sup>b</sup>
120	4.55 ± 0.12	3.83 ± 0.08 <sup>a</sup>	3.71 ± 0.14 <sup>a</sup>	15.78 ± 0.01	18.48 ± 0.04 <sup>b</sup>
180	4.90 ± 0.101	3.44 ± 0.04 <sup>a</sup>	3.17 ± 0.07 <sup>a</sup>	30.61 ± 0.03	35.45 ± 0.22 <sup>b</sup>
240	5.37 ± 0.189	3.21 ± 0.03 <sup>a</sup>	3.02 ± 0.03 <sup>a</sup>	40.29 ± 0.10	43.78 ± 0.04 <sup>b</sup>
300	6.02 ± 0.16	3.048 ± 0.042 <sup>a</sup>	2.863 ± 0.61 <sup>a</sup>	49.31 ± 0.18	59.64 ± 0.17 <sup>b</sup>
360	6.44 ± 0.03	2.671 ± 0.01 <sup>a</sup>	2.138 ± 0.03 <sup>a</sup>	58.16 ± 0.03	66.14 ± 0.04 <sup>b</sup>

All values are expressed as mean ± S.D., n = 6

<sup>a</sup>Significant (p < 0.05) compared to control

<sup>b</sup>Significant (p < 0.05) compared to pure drug (ketoprofen)

volume of control groups. The paw edema volume estimates (before and after drug administration) and % inhibition of edema at different time interval was persuaded and displayed in Table 4. The co-crystal and ketoprofen unveiled inhibition of paw edema as 66.14 ± 0.04% and 58.16 ± 0.03% at the end of 6 h, respectively thus demonstrating quick onset of action by co-crystal in contrast with the pure drug ketoprofen.

**Statistical analysis** Data were compared by ANOVA followed by Tukey’s test. The p value is <0.0005 is considered as significant.

### Analgesic activity

The results of the % analgesic activity (PAA) of test, reference and control group are shown in Table 5. The PAA (Eq. (9)) was comparatively evaluated for KP-PABA co-crystal and pure drug based on its potential to suppress pain. KP-PABA co-crystal showed significant effect in enhancing the pain threshold to a certain extent when compared to that of drug (ketoprofen), thus, stipulating that an improvement in solubility further tweaked the pharmacological response.

## Conclusion

Ketoprofen-p-aminobenzoic acid co-crystal were prepared by solvent evaporation technique employing central composite experimental design. The optimized batch containing ketoprofen and PABA in molar ratio (1:1) after characterization by FT-IR, XRD, DSC, SEM, and NMR studies was further evaluated for in-vitro and in-vivo anti-inflammatory and analgesic activities. The solubility and % drug release of different batches of co-crystal was found to be between 34.20–60.11 µg/ml and 68.11–93.45%, respectively. The results of in-vivo anti-inflammatory activity by rat paw edema method provided a significant % inhibition in paw



**Table 5** Percent analgesic effect of ketoprofen and KP-PABA by tail flick method in mice

Treatment	PAA					
	0 h	1 h	2 h	3 h	4 h	5 h
Standard (ketoprofen)	0.03 ± 0.007	31.30 ± 0.92 <sup>a</sup>	35.18 ± 1.09 <sup>a</sup>	42.36 ± 0.82 <sup>a</sup>	50.93 ± 0.96 <sup>a</sup>	71.96 ± 0.76 <sup>a</sup>
Test (KP-PABA co-crystal)	0.02 ± 0.008	35.51 ± 1.02 <sup>a,b</sup>	48.63 ± 1.17 <sup>a,b</sup>	55.84 ± 0.90 <sup>a,b</sup>	67.82 ± 0.85 <sup>a,b</sup>	78.92 ± 0.88 <sup>a,b</sup>
Control (vehicle)	0.01 ± 0.01	0.91 ± 0.27	1.32 ± 0.12	0.83 ± 0.29	1.1 ± 0.24	0.021 ± 0.01

All values are expressed as mean ± S.D.,  $n = 6$

<sup>a</sup>Significant ( $p < 0.001$ ) compared to control

<sup>b</sup>Significant ( $p < 0.001$ ) compared to pure drug (ketoprofen)

volume by co-crystal formulation as compared to standard drug in wistar rats whereas in-vivo analgesic activity further showed that pain threshold has significantly enhanced. The  $IC_{50}$  value of co-crystal formulation is almost half as compared to pure drug. Hence, it is concluded that co-crystal formulation is more active in producing anti-inflammatory response than the drug ketoprofen. On that account, it can be concluded that co-crystallization proves to be a promising technique for enhancing the solubility characteristics of BCS -II drugs.

## Materials and methods

### Materials

Ketoprofen (KP) was obtained from Infinity Laboratories Pvt. Ltd (Behra, India). *p*-aminobenzoic acid (PABA) was supplied by Central Drug House (P) Ltd., New Delhi. Sodium chloride, acetic acid, carrageenan, ethanol, disodium hydrogen orthophosphate, potassium di-hydrogen orthophosphate was procured from Hi-Media lab. Pvt. Ltd. All other chemicals & reagents used in the study were of analytical grade and used as received.

### Methods

#### Synthesis of ketoprofen-*p*-aminobenzoic acid (KP-PABA) co-crystal

Ketoprofen-*p*-aminobenzoic acid (KP-PABA) co-crystal was prepared by the solvent evaporation method as reported earlier [43]. Ketoprofen and PABA were used in stoichiometrically equal ratio and after carefully weighing were dissolved in 10 mL of acetic acid in a sealed flask and is kept under continuous stirring on a magnetic stirrer for 2 h while maintaining the temperature at 60 °C. The clear solution so formed was then filtered through 5 µm filter paper and allowed to evaporate slowly at room temperature under a fume hood.

#### Experimental design for the preparation of KP-PABA co-crystal

The preparation of co-crystal using ketoprofen and PABA was optimized using 2-factor, 3 level CCD. The concentration of ketoprofen (254.29–508.58 mg) ( $X_1$ ) and concentration of PABA (137.14–274.28 mg) ( $X_2$ ) were designated as formulation variables whereas the % drug release and solubility (µg/ml) were picked as response variables (Table 1). Each independent variable was considered at three levels (i.e. -1, 0, and 1).

#### Solubility studies

Ketoprofen pure drug and each batch of KP-PABA co-crystal formulations containing ketoprofen equivalent to 10 mg was dispersed in 10 ml of distilled water and physiological buffer (pH 7.4), separately and were kept on continuous shaking for 48 h for equilibration at room temperature (25 °C) to determine the solubility of ketoprofen. The obtained solution was filtered by 0.45 µm millipore filter paper and the drug content was determined by taking absorbance at 260 nm using uv-vis spectrophotometer. The amount of drug was calculated using the calibration curve in water. The Gibbs free energy of transfer ( $\Delta G$ ) of ketoprofen present in different batches of co-crystal is determined using Eq. (4).

$$\Delta G = -2.303RT \cdot \log \cdot S_o/S_s \quad (4)$$

$S_o$  is the solubility of the co-crystal in water and  $S_s$  is the solubility of pure drug in water,  $R = 8.31 \text{ J k}^{-1}\text{mol}^{-1}$  and  $T = 298.15 \text{ }^\circ\text{C}$ .

#### Determination of drug content

The different batches of KP-PABA co-crystal formulations containing drug equivalent to 5 mg were dissolved separately in 25 ml of phosphate buffer (pH 7.4). The samples were filtered through 0.45 µm milipore filters and after appropriate dilution the samples were analyzed by uv-vis spectrophotometer at 260 nm [44].

Total Drug Content (TDC) was calculated by the following equation.

$$\text{Total drug content(\%)} = \frac{\text{Weight of drug in co - crystal}}{\text{Weight of co - crystal}} \times 100 \quad (5)$$

### In-vitro drug release profile

In-vitro dissolution studies were performed using USP type II dissolution apparatus. Dissolution studies of pure drug (Ketoprofen) and each batch of KP-PABA co-crystal formulation containing drug equivalent to 20 mg were conducted in 900 ml phosphate buffer (pH 7.4) at  $37 \pm 0.5$  °C with a continuous stirring speed of 50 rpm. The powder was dispersed over the dissolution medium. Aliquots of sample (5 ml) were drawn at different time intervals for 60 min and replaced with an equivalent amount of the dissolution medium to retain sink conditions during the experiment. Samples were filtered through 0.45  $\mu\text{m}$  milipore filters and the concentration of ketoprofen in the samples was determined by measuring the absorbance of the samples at a wavelength of 260 nm using the uv–vis spectrophotometer followed by determination of the mechanism of release by fitting the release rate data in various release kinetic models.

## Characterization

### Fourier transform infrared spectroscopy (FT-IR)

Ketoprofen, PABA and optimized batch of KP-PABA co-crystal formulation were exposed to FT-IR spectroscopy. FTIR spectroscopy was directed by a Perkin-Elmer, Spectrum, US spectrophotometer and the spectrum was documented in the wavelength region of  $4000 \text{ cm}^{-1}$  to  $400 \text{ cm}^{-1}$  using KBr pellet method. The method involves dispersing of sample in KBr and compressing into disc by applying a pressure of  $50 \text{ kg/cm}^2$  in hydraulic press.

### Powder X-ray diffraction (PXRD)

The ketoprofen, PABA, and optimized batch of KP-PABA co-crystal formulation powder samples were examined using an X-ray diffractometer (Miniflex 2, Rigaku, Japan) from  $0^\circ$  to  $80^\circ$  diffraction angle ( $2\theta$ ). The Miller index ( $d_{hkl}$ ) signifies direction and plane in the crystal and is determined using Bragg's equation (Eq. (6)).

$$n\lambda = 2d_{hkl} \sin\theta \quad (6)$$

here  $\lambda$  and  $n$  denote the wavelength ( $1.5418 \text{ \AA}$ ) and order ( $n = 1$ , first order), respectively;  $\theta$  is the Bragg's angle.

### Differential scanning calorimetry (DSC)

Thermal behavior of ketoprofen, PABA and optimized batch of KP-PABA co-crystal formulation was studied using a DSC (Mettler Toledo, Switzerland), heated the samples within the temperature range of  $20$ – $250$  °C with a scanning rate of  $10$  °C/min in aluminum pans under nitrogen flow at a rate of  $50 \text{ ml/min}$ .

### Scanning electron microscopy (SEM)

The surface morphology and shape of optimized batch of KP-PABA co-crystal formulation was examined using SEM (JSM-6100 scanning microscopy, Japan). The sample (optimized batch) after coated with gold was mounted on aluminum stub containing double-adhesive carbon tape. The photographs were observed at acceleration voltage of  $10 \text{ kV}$ .

### Nuclear magnetic resonance (NMR) spectroscopy

The NMR spectra of ketoprofen, PABA and optimized batch of KP-PABA co-crystal formulation after dissolving in  $\text{DMSO-d}_6$  were examined using Bruker Avance AV 400 NMR spectrometer (Bruker, Karlsruhe, Germany) to get solution  $^{13}\text{C}$  NMR data at a temperature of  $293 \text{ K}$  using Tetramethylsilane (TMS) as an internal standard [45]. Data were interpreted using Mnova program (Mestrelab Research, Santiago de Compostela, Spain).

### Stability studies

The optimized batch of co-crystal was kept for the accelerated stability studies according to ICH guidelines ( $40 \pm 2$  °C and  $75 \pm 5\%$  RH) for a period of 6 months in a stability chamber. The samples were placed in hermetically sealed vials containing rubber plugs and aluminum bung. The stored co-crystal was taken out after 6 months and evaluated for the drug content (according to the method described in earlier section of drug content,  $n = 3$ ) and for any physical changes [13].

## Biological evaluation of KP-PABA co-crystal

### In-vitro anti-inflammatory activity

Egg albumin denaturation method was employed to evaluate in-vitro anti-inflammatory activity of drug ketoprofen and optimized batch of KP-PABA co-crystal [46]. The mixture contained of pure fresh hen's egg albumin ( $0.2 \text{ ml}$ ),

Phosphate buffer saline, pH 7.4 (2.8 ml)) and different concentrations of KP-PABA co-crystal formulation (2 ml, containing ketoprofen equivalent to 10 mg) (125, 250, 500, 750 & 1000 µg/ml in Dimethyl sulfoxide as solvent). After incubation (Caltan, NSW, India) for 15 min at a temp of  $37 \pm 2$  °C, the temperature of mixture was raised to 70 °C. After cooling at room temperature, the absorbance was measured at  $\lambda_{\text{max}}$  of 660 nm. Similar procedure was followed for the model drug ketoprofen containing same concentrations as for the formulation, as a reference or control [47, 48].

The percentage protection from protein denaturation was calculated as per Eq. (7)

$$\% \text{ protection from denaturation} = \frac{\text{Absorbance of control} - \text{Absorbance of sample}}{\text{Absorbance of control}} \times 100 \quad (7)$$

The half-maximal inhibitory concentration (IC<sub>50</sub>) values of ketoprofen and optimized formulation was measured by nonlinear regression analysis.

#### In-vivo carrageenan-induced anti-inflammatory activity

The protocol with registration no. CPCSEA Reg. no-IAEC/2020/10-18 was approved for animal study by the Animal Ethical Committee, Guru Jambheshwar University of Science and Technology, Hisar, India. Wistar rats (180–210 g) of either sex were divided into three groups comprising of six animals each. Group I (Control treated) with carrageenan was kept as control, Group II (standard Drug) was treated with drug-ketoprofen (10 mg/kg) and Group III (Test compound) was treated with KP-PABA co-crystal (equivalent to ketoprofen 10 mg/kg) body weight administrated orally. 0.1 ml of 1% suspension of carrageenan in normal saline, was administered as subplantar injection in the left hind paw of albino wistar rats, after 1 h after of oral administration of the test materials. The paw volume was measured using vernier caliper at 1, 2, 3, 4, 5, and 6 h after the carrageenan injection [49, 50]. The % inhibition in paw volume was calculated by using Eq. (8)

$$\% \text{ inhibition} = \frac{V_c - V_t}{V_c} \times 100 \quad (8)$$

where  $V_c$  and  $V_t$  is the inflammatory increase in paw volume control group and the inflammatory increase in paw volume in test group respectively [51, 52].

#### Analgesic activity (Tail flick method)

Analgesic activity was measured by tail flick method using a radiant type analgesiometer. In tail flick method pain was produced by placing the tip of the tail on the heat source. Mice (25–30 g) of either sex were divided into three groups (test, standard, and control) containing six animals in each group. The tail flick reaction time for each animal was recorded six times before administering the drug and the mean was used as predrug reaction time. A dose of the standard drug (Ketoprofen) and test compound (optimized batch of KP-PABA co-crystal) containing ketoprofen equivalent to 5 mg/kg of body weight in 0.9% w/v sterile saline was administered to animals. The test and standard group received drug orally while the control group was catered with vehicle only. After administration of the drug, the tail flick reaction time was measured at different time interval as 0, 1, 2, 3, 4 and 5 h [53].

% Analgesic activity (PAA) was calculated by using the Eq. (9) below:

$$\text{PAA} = (T_2 - T_1)/T_1 * 100 \quad (9)$$

where,  $T_1$  and  $T_2$  are reaction time in seconds before and after treatment with drug, respectively. Data were analyzed by one-way ANOVA method and further followed by Tukey's post-hoc test, statistically and is denoted as  $P$  value.

**Acknowledgements** The authors are highly grateful to Department of Pharmaceutical Sciences, Central Instrumentation Laboratory and Material Science Laboratory, Guru Jambheshwar University of Science and Technology, Hisar for providing necessary facilities to carry out the research.

#### Compliance with ethical standards

**Conflict of interest** The authors declare no competing interests.

**Ethical approval** The procedure followed for animal handling is in accordance with the protocol as approved for animal study (CPCSEA Reg. no-IAEC/2020/10-18) by the Institutional Animal Ethical Committee, Guru Jambheshwar University of Science and Technology, Hisar, India.

**Publisher's note** Springer Nature remains neutral with regard to jurisdictional claims in published maps and institutional affiliations.

#### References

1. Sarraguça MC, Ribeiro PR, Dos Santos AO, Lopes JA. Batch statistical process monitoring approach to a cocrystallization

- process. *J Pharm Sci.* 2015;104:4099–108. <https://doi.org/10.1002/jps.24623>.
2. Soares FL, Carneiro RL. Green synthesis of ibuprofen–nicotinamide cocrystals and in-line evaluation by Raman spectroscopy. *Cryst Growth Des.* 2013;13:1510–7. <https://doi.org/10.1021/cg3017112>.
  3. Harriss BI, Vella-Zarb L, Wilson C, Evans IR. Furosemide cocrystals: Structures, hydrogen bonding, and implications for properties. *Cryst Growth Des.* 2014;14:783–91. <https://doi.org/10.1021/cg401662d>.
  4. Padrela L, Rodrigues MA, Velaga SP, Matos HA, de Azevedo EG. Formation of indomethacin–saccharin cocrystals using supercritical fluid technology. *Eur J Pharm Sci.* 2009;38:9–17. <https://doi.org/10.1016/j.ejps.2009.05.010>.
  5. Chow SF, Shi L, Ng WW, Leung KH, Nagapudi K, Sun CC, et al. Kinetic entrapment of a hidden curcumin cocrystal with phloroglucinol. *Cryst Growth Des.* 2014;14:5079–89. <https://doi.org/10.1021/cg5007007>.
  6. Childs SL, Stahly GP, Park A. The salt–cocrystal continuum: the influence of crystal structure on ionization state. *Mol Pharm.* 2007;4:323–38. <https://doi.org/10.1021/mp0601345>.
  7. Berry DJ, Steed JW. Pharmaceutical cocrystals, salts and multi-component systems; intermolecular interactions and property based design. *Adv Drug Deliv Rev.* 2017;117:3–24. <https://doi.org/10.1016/j.addr.2017.03.003>.
  8. da Silva CC, Pepino RD, de Melo CC, Tenorio JC, Ellena J. Controlled synthesis of new 5-fluorocytosine cocrystals based on the p K a rule. *Cryst Growth Des.* 2014;14:4383–93. <https://doi.org/10.1021/cg500502j>.
  9. Aitipamula S, Chow PS, Tan RB. Polymorphism in cocrystals: a review and assessment of its significance. *Cryst Eng Comm.* 2014;16:3451–65. <https://doi.org/10.1039/C3CE42008F>.
  10. Lee KS, Kim KJ, Ulrich J. Formation of salicylic acid/4, 4'-dipyridyl cocrystals based on the ternary phase diagram. *Chem Eng Technol.* 2015;38:1073–80. <https://doi.org/10.1002/ceat.201400738>.
  11. Shayanfar A, Jouyban A. Physicochemical characterization of a new cocrystal of ketoconazole. *Powder Technol.* 2014;262:242–8. <https://doi.org/10.1016/j.powtec.2014.04.072>.
  12. Ganesh M, Ubaidulla U, Rathnam G, Jang HT. Chitosan–telmisartan polymeric cocrystals for improving oral absorption: In vitro and in vivo evaluation. *Int J Biol Macromol.* 2019;131:879–85. <https://doi.org/10.1016/j.ijbiomac.2019.03.141>.
  13. Mutalik S, Anju P, Manoj K, Usha AN. Enhancement of dissolution rate and bioavailability of aceclofenac: a chitosan-based solvent change approach. *Int J Pharm.* 2008;350:279–90. <https://doi.org/10.1016/j.ijpharm.2007.09.006>.
  14. Alvani A, Jouyban A, Shayanfar A. The effect of surfactant and polymer on solution stability and solubility of tadalafil–methylparaben cocrystal. *J Mol Liq.* 2019;281:86–92. <https://doi.org/10.1016/j.molliq.2019.02.080>.
  15. Rahman Z, Agarabi C, Zidan AS, Khan SR, Khan MA. Physico-mechanical and stability evaluation of carbamazepine cocrystal with nicotinamide. *AAPS Pharm Sci Tech.* 2011;12:693–704. <https://doi.org/10.1208/s12249-011-9603-4>.
  16. Lyn LY, Sze HW, Rajendran A, Adinarayana G, Dua K, Garg S. Crystal modifications and dissolution rate of piroxicam. *Acta Pharm.* 2011;61:391–402. <https://doi.org/10.2478/v10007-011-0037-z>.
  17. Zhang YX, Wang LY, Dai JK, Liu F, Li YT, Wu ZY, et al. The comparative study of cocrystal/salt in simultaneously improving solubility and permeability of acetazolamide. *J Mol Str.* 2019;1184:225–32. <https://doi.org/10.1016/j.molstruc.2019.01.090>.
  18. Gautam MK, Besan M, Pandit D, Mandal S, Chadha R. Cocrystal of 5-fluorouracil: characterization and evaluation of biopharmaceutical parameters. *AAPS Pharm Sci Tech.* 2019;20:1–7. <https://doi.org/10.1208/s12249-019-1360-9>.
  19. Kaleemullah M, Jiyauddin K, Thiban E, Rasha S, Al-Dhali S, Budiasih S, et al. Development and evaluation of Ketoprofen sustained release matrix tablet using Hibiscus rosa-sinensis leaves mucilage. *Saudi Pharm J.* 2017;25:770–9. <https://doi.org/10.1016/j.jpsps.2016.10.006>.
  20. Rençber S, Karavana SY, Özyazici M. Bioavailability file: ketoprofen. *FABAD J Pharm Sci.* 2009;34:203.
  21. Bhatia M, Devi S. Development, characterisation and evaluation of PVP K-30/PEG solid dispersion containing ketoprofen. *ACTA Pharm Sci.* 2020;58. <https://doi.org/10.23893/1307-2080.APS.05806>.
  22. Bhatia M, Devi R. Enhanced solubility and drug release of ketoprofen using lyophilized bovine serum albumin solid dispersion. *ACTA Pharm Sci.* 2019;57. <https://doi.org/10.23893/1307-2080.APS.05703>.
  23. Hezave AZ, Aftab S, Esmaeilzadeh F. Micronization of ketoprofen by the rapid expansion of supercritical solution process. *J Aerosol Sci.* 2010;41:821–33.
  24. Vittal GV, Deveswaran R, Bharath S, Basavaraj BV, Madhavan V. Formulation and characterization of ketoprofen liquisolid compacts by Box-Behnken design. *Int J Pharm Investig.* 2012;2:150. <https://doi.org/10.4103/2230-973X.104398>.
  25. Nikumbh KV, Sevankar SG, Patil MP. Formulation development, in vitro and in vivo evaluation of microemulsion-based gel loaded with ketoprofen. *Drug Deliv.* 2015;22:509–15. <https://doi.org/10.3109/10717544.2013.859186>.
  26. Ambala R, Vemula SK. Formulation and characterization of ketoprofen emulgels. *J Appl Pharm Sci.* 2015;5:112–7. <https://doi.org/10.7324/JAPS.2015.50717>.
  27. Attia MF, Anton N, Khan IU, Serra CA, Messaddeq N, Jakhmola A, et al. One-step synthesis of iron oxide polypyrrole nanoparticles encapsulating ketoprofen as model of hydrophobic drug. *Int J Pharm.* 2016;508:61–70. <https://doi.org/10.1016/j.ijpharm.2016.04.073>.
  28. Gul R, Ahmed N, Ullah N, Khan MI, Elaissari A. Biodegradable ingredient-based emulgel loaded with ketoprofen nanoparticles. *AAPS Pharm Sci Tech.* 2018;19:1869–81. <https://doi.org/10.1208/s12249-018-0997-0>.
  29. Kheradmandnia S, Vasheghani-Farahani E, Nosrati M, Atyabi F. Preparation and characterization of ketoprofen-loaded solid lipid nanoparticles made from beeswax and carnauba wax. *NANOMED- Nanotechnol.* 2010;6:753–9. <https://doi.org/10.1016/j.nano.2010.06.003>.
  30. Xi MM, Wang XY, Fang KQ, Gu Y. Study on the characteristics of pectin–ketoprofen for colon targeting in rats. *Int J Pharm.* 2005;298:91–7. <https://doi.org/10.1016/j.ijpharm.2005.04.012>.
  31. Kluge J, Fusaro F, Casas N, Mazzotti M, Muhrer G. Production of PLGA micro- and nanocomposites by supercritical fluid extraction of emulsions: I. Encapsulation of lysozyme. *J Supercrit Fluids.* 2009;50:327–35. <https://doi.org/10.1016/j.supflu.2009.05.002>.
  32. Perpétuo GL, Chierice GO, Ferreira LT, Fraga-Silva TF, Venturini J, Arruda MS, et al. A combined approach using differential scanning calorimetry with polarized light thermomicroscopy in the investigation of ketoprofen and nicotinamide cocrystal. *Thermochim Acta.* 2017;651:1–0. <https://doi.org/10.1016/j.tca.2017.02.014>.
  33. Maheshwari C, André V, Reddy S, Roy L, Duarte T, Rodríguez-Hornedo N. Tailoring aqueous solubility of a highly soluble compound via cocrystallization: effect of coformer ionization, pH max and solute–solvent interactions. *Cryst Eng Comm.* 2012;14:4801–11. <https://doi.org/10.1039/C2CE06615G>.
  34. Sathisaran I, Dalvi SV. Engineering cocrystals of poorly water-soluble drugs to enhance dissolution in aqueous medium. *Pharmaceutics.* 2018;10:108. <https://doi.org/10.3390/pharmaceutics10030108>.

35. Sanphui P, Kumar SS, Nangia A. Pharmaceutical cocrystals of niclosamide. *Cryst Growth Des.* 2012;12:4588–99. <https://doi.org/10.1021/cg300784v>.
36. Bhogala BR, Basavoju S, Nangia A. Tape and layer structures in cocrystals of some di- and tricarboxylic acids with 4,4'-bipyridines isonicotinamide Bin ternary cocrystals. *Cryst Eng Comm.* 2005;7:551–62. <https://doi.org/10.1039/B509162D>.
37. Sun S, Zhang X, Cui J, Liang S. Identification of the Miller indices of a crystallographic plane: a tutorial and a comprehensive review on fundamental theory, universal methods based on different case studies and matters needing attention. *Nanoscale.* 2020;12:16657–77. <https://doi.org/10.1039/D0NR03637D>.
38. Yadav AV, Shete AS, Dabke AP, Kulkarni PV, Sakhare SS. Cocrystals: a novel approach to modify physicochemical properties of active pharmaceutical ingredients. *Indian J Pharm Sci.* 2009;71:359. <https://doi.org/10.4103/0250-474X.57283>.
39. Stewart JJ. *Stewart Computational Chemistry, MOPAC2016.* Colorado Springs. 2016; <http://OpenMOPAC.net>.
40. Granovsky AA. Firefly version 8, <http://classic.chem.msu.su/gran/firefly/index.html>.
41. Lu T, Chen F. Multiwfn: a multifunctional wavefunction analyzer. *J Comput Chem.* 2012;33:580–92. <https://doi.org/10.1002/jcc.22885>.
42. Humphrey W, Dalke A, Schulten K. VMD: visual molecular dynamics. *J Mol Graph.* 1996;14:33–8. [https://doi.org/10.1016/0263-7855\(96\)00018-5](https://doi.org/10.1016/0263-7855(96)00018-5).
43. Sarkar A, Rohani S. Cocrystals of acyclovir with promising physicochemical properties. *J Pharm Sci.* 2015;104:98–105. <https://doi.org/10.1002/jps.24248>.
44. Farrag Y, Ide W, Montero B, Rico M, Rodríguez-Llamazares S, Barral L, et al. Preparation of starch nanoparticles loaded with quercetin using nanoprecipitation technique. *Int J Biol Macromol.* 2018;114:426–33. <https://doi.org/10.1016/j.ijbiomac.2018.03.134>.
45. Luo Y, Chen S, Zhou J, Chen J, Tian L, Gao W, et al. Luteolin cocrystals: characterization, evaluation of solubility, oral bioavailability and theoretical calculation. *J Drug Deliv Sci Technol.* 2019;50:248–54. <https://doi.org/10.1016/j.jddst.2019.02.004>.
46. Chavan RR, Hosamani KM. Microwave-assisted synthesis, computational studies and antibacterial/anti-inflammatory activities of compounds based on coumarin-pyrazole hybrid. *R Soc Open Sci.* 2018;5:172435. <https://doi.org/10.1098/rsos.172435>.
47. Alshaikh RA, Essa EA, El Maghraby GM. Eutexia for enhanced dissolution rate and anti-inflammatory activity of nonsteroidal anti-inflammatory agents: caffeine as a melting point modulator. *Int J Pharm.* 2019;563:395–405. <https://doi.org/10.1016/j.ijpharm.2019.04.024>.
48. Shandil A, Yadav M, Sharma N, Nagpal K, Jindal DK, Deep A, et al. Targeting keratinocyte hyperproliferation, inflammation, oxidative species and microbial infection by biological macromolecule-based chitosan nanoparticle-mediated gallic acid–rutin combination for the treatment of psoriasis. *Polym Bull.* 2020;77:4713–38. <https://doi.org/10.1007/s00289-019-02984-9>.
49. Komakech R, Kim YG, Matsabisa GM, Kang Y. Anti-inflammatory and analgesic potential of *Tamarindus indica* Linn. (Fabaceae): a narrative review. *Integr Med Res.* 2019;8:181–6. <https://doi.org/10.1016/j.imr.2019.07.002>.
50. Mondal A, Maity TK, Bishayee A. Analgesic and anti-inflammatory activities of quercetin-3-methoxy-4'-glucosyl-7-glucoside isolated from Indian medicinal plant *Melothria heterophylla*. *Medicines.* 2019;6:59. <https://doi.org/10.3390/medicines6020059>.
51. Khullar R, Kumar D, Seth N, Saini S. Formulation and evaluation of mefenamic acid emulgel for topical delivery. *Saudi Pharma J.* 2012;20:63–7. <https://doi.org/10.1016/j.jsps.2011.08.001>.
52. Olbert M, Gdula-Argasińska J, Nowak G, Librowski T. Beneficial effect of nanoparticles over standard form of zinc oxide in enhancing the anti-inflammatory activity of ketoprofen in rats. *Pharmacol Rep.* 2017;69:679–82.
53. Kulkarni SK. Heat and other physiological stress-induced analgesia: catecholamine mediated and naloxone reversible response. *Life Sci.* 1980;27:185–8. [https://doi.org/10.1016/0024-3205\(80\)90136-8](https://doi.org/10.1016/0024-3205(80)90136-8).